ISBN: 978-3-95450-224-0 ISSN: 2673-7035 doi:10.18429/JACoW-FLS2023-TU4P18

NONLINEAR DYNAMICS MEASUREMENTS AT THE EBS STORAGE RING

N. Carmignani*, L. Carver, L. Hoummi, S. Liuzzo, T. Perron, S. White
ESRF, Grenoble, France

Abstract

The Extremely Brilliance Source (EBS) is a 4th generation synchrotron light source and it has been in user operation since August 2020 at the ESRF. Several measurements to characterise the nonlinear dynamics have been performed in 2023: nonlinear chromaticity, second order dispersion and detuning with amplitude. The results of the measurements are shown and compared with simulations.

INTRODUCTION

The EBS has been in user operation since August 2020 at the ESRF [1]. The nonlinear dynamics model of the storage ring has been improved by adding the cross talk effect of some magnets to their neighbors [2]. The Touschek lifetime of the machine reached the design values already in the first year of user operation [3] and it is improved regularly by online nonlinear optimization [4]. The horizontal dynamic aperture and therefore the injection efficiency is still slightly lower than the one predicted by the model [3].

In order to better understand the disagreement with the model of the horizontal dynamic aperture, in 2023 we performed a series of nonlinear dynamics measurements and we compared them with the accelerator model.

In the next section we will show the measurements of transverse detuning with amplitude and in the following the measurements of high order chromaticity and second order dispersion. For all the cases, a comparison with the theoretical model is shown.

DETUNING WITH AMPLITUDE

Measurement Technique

In order to measure the detuning with amplitude we need to excite coherent oscillations of the beam at increasing amplitudes and measure the frequency of the free oscillations.

A kicker magnet able to excite the beam for about 1 turn, either in horizontal or vertical, will be installed in the ESRF-EBS storage ring in 2024. The four injection kickers can be used to excite horizontally the beam, but their field has a raising time of about 70 µs (see Fig. 1) [5]. The four injection kickers are usually pulsed with a current of about 1.6 to 1.9 kA.

Since the pulsed power supplies limit the minimum sent currents to a few hundreds of Amperes, we excited the beam by powering all the four kickers at full current except for the kicker K3, that was powered with reduced current. The described distribution of currents generates a bump that is not perfectly closed. In Fig. 2, the turn by turn (TBT) orbit

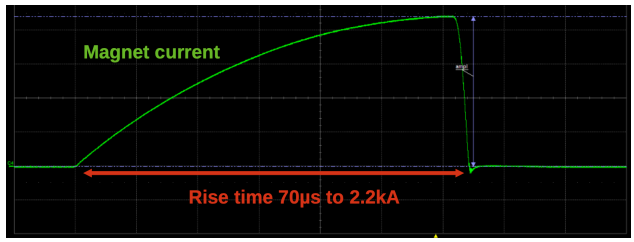

Figure 1: Pulse shape of the injection kickers.

in the first beam position monitor (BPM), which is located inside the injection bump, is shown for different current reductions of the kicker K3 power supply. The injection oscillations are dumped in about 100 turns because of the decoherence due to the high chromaticity. The radiation damping is a slower effect that lasts a few thousands turns.

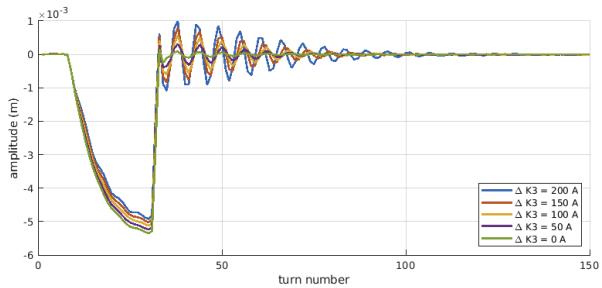

Figure 2: Orbit at the BPM number 1, which is inside the injection bump, during the ramp rise and after it goes off in about 1 turn. The oscillations are dumped quickly because of strong decoherence due to the high chromaticity.

The tune is extracted from the first 130 turns of oscillations using 5 consecutive measurements in all the 320 BPM. In order to increase the resolution of the FFT, a zero-padding of the signal with 12000 samples has been added to the measurements. A histogram of the 320 x 5 tune measurements for a single amplitude is shown in Fig. 3. The standard deviation of the histogram is about 5×10^{-4} and it is considered as the measurement error for the tune. From the peak to peak oscillation amplitude at each BPM, knowing the beta functions, we can extract the action of the beam and compute the tune shift with amplitude.

The vertical tune can be measured in the same way. Even if the injection kickers produce a horizontal excitation, some smaller vertical oscillations can be observed and can be used to measure the vertical tune as a function of horizontal amplitude of oscillations.

* nicola.carmignani@esrf.fr

ISBN: 978-3-95450-224-0 ISSN: 2673-7035 doi:10.18429/JACoW-FLS2023-TU4P18

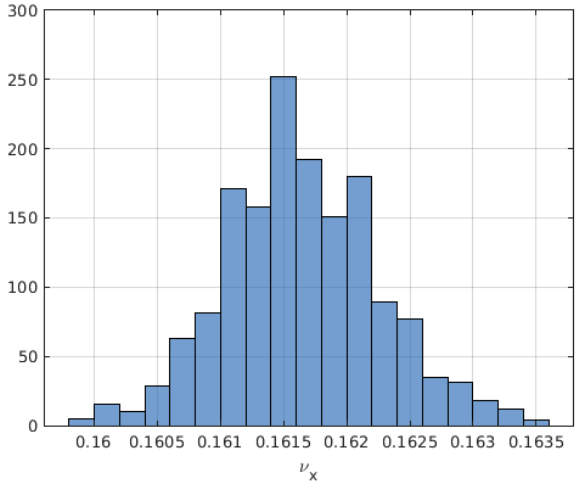

Figure 3: Histogram of the 320 x 5 measurements of the horizontal tune taken from the 320 BPMs in 5 consecutive acquisitions.

Comparison with Accelerator Model

The tune shift with amplitude has been measured for three different octupole settings: the nominal setting, which is a result of online optimizations to maximise the Touschek lifetime [4], and two settings with octupoles powered at 50% and 10% of the nominal strength.

Figures 4 and 5 show the comparison between the measured and simulated tune shift with amplitude: the first is the horizontal tune shift with horizontal amplitude and the second is the vertical tune shift with horizontal amplitude.

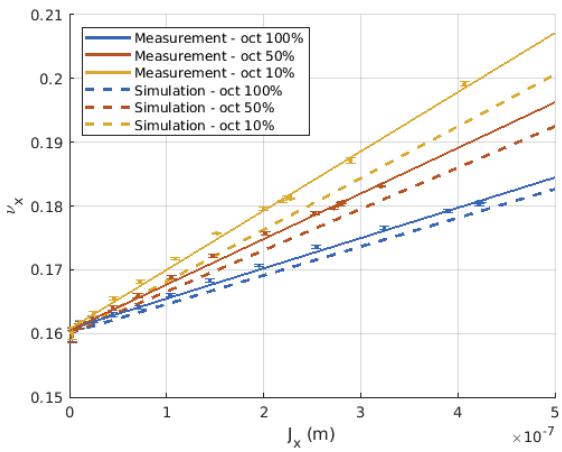

Figure 4: Horizontal tune shift with horizontal amplitude. The solid lines are the fit of the measured data, the dashed lines are from simulations.

The detuning with amplitude measurements are summarised in Tables 1 and 2. For the horizontal tune shift with horizontal amplitude, the measured value is larger than the expected by about 10%. The measurement of the vertical tune shift with horizontal amplitude disagrees with the model by about a factor 2. This disagreement is an indication of a problem in the nonlinear model of the EBS storage ring.

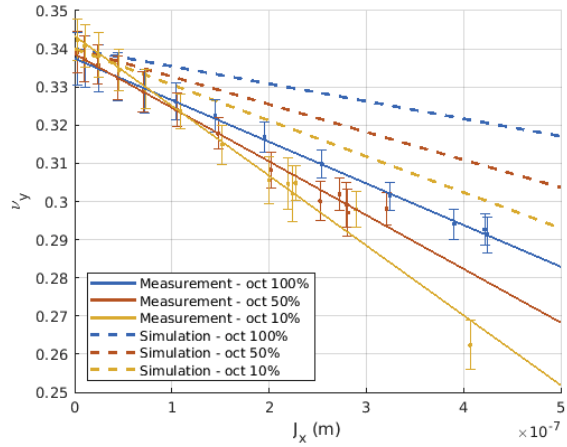

Figure 5: Vertical tune shift with horizontal amplitude. The solid lines are the fit of the measured data, the dashed lines are from simulations.

Table 1: Measurements and simulations of horizontal detuning with amplitude.

Octupoles Fraction	**Sim.** $d\nu_x/dJ_x$ (10^{-4} m^{-1})	**Meas.** $d\nu_x/dJ_x$ (10^{-4} m^{-1})
10%	7.93	9.3 ± 0.3
50%	6.35	7.1 ± 0.3
100%	4.35	4.7 ± 0.2

Table 2: Measurements and simulations of vertical detuning with horizontal amplitude.

Octupoles Fraction	**Sim.** $d\nu_x/dJ_x$ (10^{-4} m^{-1})	**Meas.** $d\nu_x/dJ_x$ (10^{-4} m^{-1})
10%	-8.95	-18 ± 2
50%	-6.84	-14 ± 1
100%	-4.20	-10.9 ± 0.3

HIGH ORDER CHROMATICITY

The second order chromaticity can be measured by performing a third order polynomial fit of the horizontal and vertical tunes as a function of energy deviation. The energy of the machine has been changed by changing the RF frequency, using Eq. (1). The RF frequency has been changed from -300 Hz to +500 Hz.

$$\frac{dp}{p} = -\frac{1}{\alpha}\frac{df}{f} \quad (1)$$

In Fig. 6, the horizontal tunes as a function of energy deviation are shown for the three different octupole settings. The measurements are compared to the simulation, where

ISBN: 978-3-95450-224-0 ISSN: 2673-7035 doi:10.18429/JACoW-FLS2023-TU4P18

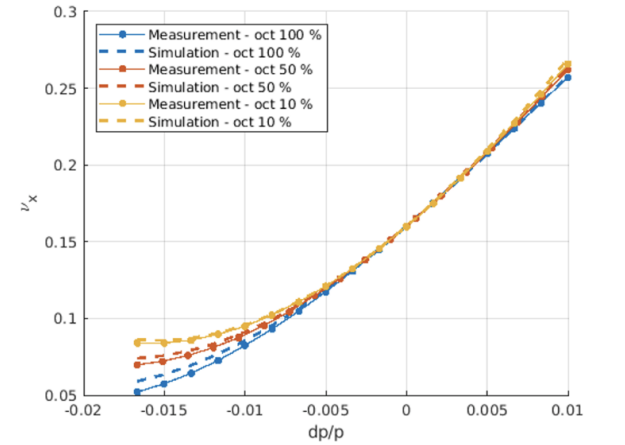

Figure 6: Horizontal tunes as a function of energy deviation. The dots are the measured point and the dashed line is the simulation.

the linear part of the chromaticity has been matched to the measured value (9.1, 9.2). All the measured and simulated values are summarised in Table 3.

Table 3: Measurements and simulations of second order chromaticities.

Octupoles Fraction	$1/2\,\mathrm{d}^2\nu_x/\mathrm{d}\delta^2$ **Sim.**	**Meas.**	$1/2\,\mathrm{d}^2\nu_y/\mathrm{d}\delta^2$ **Sim.**	**Meas.**
10%	117.4	98 ± 1	130.6	145 ± 2
50%	176.4	157 ± 1	89.8	101 ± 1
100%	223.7	206 ± 1	57.1	68 ± 1

The second order chromaticities disagree with the model by 10% to 20% both in horizontal and in vertical.

SECOND ORDER DISPERSION

The second order dispersion can be measured at the same time of the nonlinear chromaticity. The orbit in the 320 BPMs has been acquired for each point of energy deviation and then a third order polynomial fit has been performed for each BPM.

Figure 7 shows an example of measured and simulated orbits in a BPM. The second order dispersion is the parabolic component. The result of the fit depends on the order of the polynomial that we decide to use and can be affected by the nonlinearities of the BPMs at large amplitude.

In Fig. 8, the measured and the simulated second order dispersions are shown for the three octupole settings. In simulation, the second order dispersion does not depend on the octupole settings, while in the measurement it can change by almost a factor 2.

The disagreement between measurement and simulation is larger, more than a factor 2, when the octupoles have the full strength.

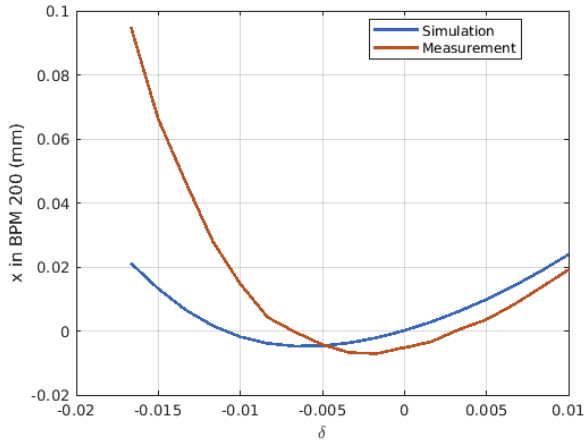

Figure 7: Horizontal orbit in BPM number 200 as a function of energy deviation with octupoles at 10% of their nominal strengths. The measured second order dispersion is about a factor 2 larger than the simulated.

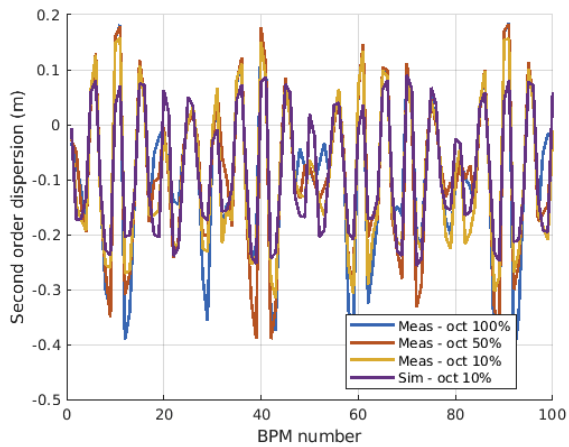

Figure 8: Measured second order dispersion for three octupole settings and simulated value.

CONCLUSION

The detuning with amplitude of the EBS storage ring is close to the predicted one for the horizontal case, within a 10% error, but the cross term is off by almost a factor 2. The vertical detuning could not be measured without a vertical kicker.

The second order chromaticities are about 10% to 20% far from the prediction of the model.

The measured second order dispersion depends unexpectedly on the octupole setting and it is in disagreement with the model by more than a factor 2 in some locations.

ISBN: 978-3-95450-224-0 ISSN: 2673-7035 doi:10.18429/JACoW-FLS2023-TU4P18

REFERENCES

[1] P. Raimondi *et al.*, "The extremely brilliant source storage ring of the european synchrotron radiation facility," *Communications Physics*, vol. 6, no. 1, p. 82, 2023. doi:10.1038/s42005-023-01195-z

[2] G. Le Bec, J. Chavanne, S. Liuzzo, and S. White, "Cross talks between storage ring magnets at the extremely brilliant source at the european synchrotron radiation facility," *Phys. Rev. Accel. Beams*, vol. 24, no. 7, p. 072 401, 2021. doi:10.1103/PhysRevAccelBeams.24.072401

[3] P. Raimondi *et al.*, "Commissioning of the hybrid multibend achromat lattice at the european synchrotron radiation facility," *Phys. Rev. Accel. Beams*, vol. 24, no. 11, p. 110 701, 2021. doi:10.1103/PhysRevAccelBeams.24.110701

[4] N. Carmignani *et al.*, "Online optimization of the ESRF-EBS storage ring lifetime," in *Proc. IPAC'22*, Bangkok, Thailand, 2022, pp. 2552–2555. doi:10.18429/JACoW-IPAC2022-THPOPT001

[5] S. White *et al.*, "Commissioning of new kicker power supplies to improve injection perturbations at the ESRF," in *Proc. IPAC'22*, Bangkok, Thailand, 2022, pp. 2683–2685. doi:10.18429/JACoW-IPAC2022-THPOPT041